



Manufacturing Letters

Manufacturing Letters 00 (2023) 000-000



51st SME North American Manufacturing Research Conference (NAMRC 51, 2023)

Tool wear area estimation through in-process edge force coefficient in trochoidal milling of Inconel 718

Aash M Shaha, Ankit Agarwala,*, Laine Mearsa

^aInternational Center for Automotive Research, Clemson University, Greenville, SC 29607

Abstract

The rapid wear and premature failure of the cutting tool are prone to happen due to increased forces during machining difficult-to-cut materials such as Inconel 718. The application of alternative toolpath such as trochoidal milling has significantly improved tool life and reduced the overall cycle time of the process. The wear pattern of the tool has a direct impact on the cutting forces, which increases with tool deterioration. The cutting forces in milling are modeled through the mechanistic force model and can be designated through a set of force coefficients, i.e. cutting and edge representing the shearing and ploughing phenomenon of metal removal. It has been established in the literature that tool wear has a considerable effect on the value of edge force coefficients. This paper aims to determine the in-process edge force coefficients for the trochoidal toolpath and correlates them with the corresponding flank wear area. The proposed correlation will further assist in predicting the level of flank wear area based on the force values in trochoidal milling.

© 2023 Society of Manufacturing Engineers (SME). Published by Elsevier Ltd. All rights reserved. This is an open access article under the CC BY-NC-ND license (http://creativecommons.org/licenses/by-nc-nd/4.0/) Peer-review under responsibility of the Scientific Committee of the NAMRI/SME..

Keywords: Tool wear area; Trochoidal milling; Force coefficients; Inconel 718

1. Introduction

Nickel-based superalloys such as Inconel 718 have numerous applications in the aerospace and power generation industries due to their properties of high strength and resistance to thermal and corrosion effects [1]. However, these advantageous properties of Inconel 718 make it difficult to machine and result in rapid tool wear and high process forces. This rapid wear of the tool further leads to poor machinability and lower quality of the surface generated. To overcome these difficulties in the machining of Inconel 718, alternative toolpath strategies such as trochoidal toolpath [2], variable cutting speed [3], and up or down milling [4] have been investigated. The trochoidal toolpath has proven its ability to reduce tool wear and improve machinability. In the trochoidal toolpath, at any instant only a certain section of the cutter removes the material and enables rapid dissipation of heat.

Also, the continuous variation in the tool-workpiece engagement ensures reduction of high cutting loads [5]. Also, it is essential to have a practical methodology for monitoring tool conditions and to save on high costs for manufacturers. In recent times, the monitoring of tool conditions has attracted considerable interest due to the evolution of industry 4.0. The accurate estimation of tool wear in real-time can enable manufacturers or operators to utilize tools optimally and decide effectively on tool replacement. The present research work attempts to monitor the in-process progression of the flank wear area of the tool during trochoidal machining of Inconel 718.

In the past several years, numerous direct and indirect approaches have been introduced for monitoring tool condition. The direct approaches evaluate tool condition in terms of flank wear width [6] or area [7] by observing any variation in the appearance or geometry of the tool at regular intervals. The wear of the tool is interpreted by capturing quality images of the tool using an optical sensor [8], camera [9] or microscope [7]. Generally, direct approaches provide a more accurate value of tool wear parameters but tend to interrupt the cutting operation and

^{*} Corresponding author. Tel.: +1-864-990-8230. *E-mail address:* agarwa3@clemson.edu (Ankit Agarwal).

result in a loss of production time. Alternatively, the indirect approaches evaluate tool conditions by employing different sensors that monitor machining attributes, such as cutting force [10], vibrations [11], temperature [12], power [13], acoustic emission [14], etc. The idea of indirect approaches is to formulate a relationship between these machining attributes and the parameters evaluating tool wear. The indirect approaches enable a means of in-process monitoring of tool conditions and overcome the limitation of direct approaches. Also, the fusion of multiple sensors can further improve the performance of monitoring system [15]. However, the accuracy of these approaches largely depends on the correctness of the relationship formulated between the monitoring attributes and tool wear evaluation parameters.

Among all the sensing techniques of indirect approaches mentioned above, cutting force has been most commonly used for monitoring the tool condition [16]. However, the magnitude of cutting forces varies considerably with the cutting condition and can only be effective under the region of steady wear rate or dedicated cutting parameters. Cutting force is the primary reason for most tool-related faults in the milling operation and has been studied comprehensively in the literature. The mechanistic model is mainly employed to analyze cutting forces and depends on the empirically determined force coefficients [17, 18]. In the recent past, several researchers have analyzed these force coefficients to demonstrate their sensitivity towards tool wear. Choudhury and Rath [19] established a relationship between flank wear and tangential cutting force coefficients for an end milling operation. Cui [20] developed a similar relationship for the drilling operation to monitor the tool wear and showed the effective correlation exists between tangential cutting force coefficients and tool wear. Nouri et al. [21] introduced a novel method of identifying force coefficients independent of cutting conditions and used them to monitor the tool wear in real-time. Zhu and Yu [22] extended this model to high-speed milling and presented the concept of adaptable force coefficients for the modelling of force and tool wear. Subsequently, Liu et al. [23] determined the in-process force coefficients for toolpaths having varying radial immersion or feed rates and used them to monitor the tool wear. Recently, Luo et al. [24] presented a comparative assessment of various approaches to estimate tool wear through force coefficients. It was concluded that force coefficients have great potential in assessing tool wear because of lower variation in their values over the change in cutting condition.

Based on the literature review, it is realized that the application of force coefficients for estimating tool wear have not been studied for trochoidal toolpath. Also, the majority of the studies simply monitors the progression of force coefficients and outputs the wear stages (initial, steady or failure) of the tool. Further, the studies only monitor flank wear width and does not aims to estimate flank wear area of the tool, which can be an important parameter while machining of difficult-to-machine material using trochoidal toolpath [7]. The present study aims to establish a relationship that estimates real-time flank wear area using the in-process force coefficients for a trochoidal toolpath. The study uses an image recognition-based methodology to estimate flank wear area experimentally. The linear relationship established

between force coefficients and flank wear area is validated by conducting experiments at varying surface speeds.

2. Determination of cutting and edge coefficient in trochoidal toolpath

The mechanistic model correlates the uncut chip area with the elemental cutting force using cutting (K_t, K_r) and edge force coefficients (K_{te}, K_{re}) [25]. The tangential (F_t) and radial (F_r) cutting force at any instant t can be expressed using Eqs. (1) and (2). The magnitude of axial (F_a) cutting force is very less in comparison to (F_t) and (F_r) during milling with flat end cutter and it is not considered in the present study. The uncut chip area is evaluated as a multiplication of uncut chip thickness (h(t)) and axial depth of cut (b). The h(t) is defined as the shortest distance between two successive passes at any time instant t and can be calculated geometrically as explained in subsection 2.1.

$$F_t(t) = K_t b h(t) + K_{te} b \tag{1}$$

$$F_r(t) = K_r b h(t) + K_{re} b \tag{2}$$

The K_t and K_r represent the shearing/ploughing force required to generate chips, whereas K_{te} and K_{re} represents the sliding frictional/rubbing force owing to tool wear. These force coefficients are determined for a particular combination of tool and workpiece by conducting experiments. The slot cutting experiments are performed to measure cutting forces $(F_x(t), F_y(t))$ at any time instant (t) in the machine or dynamometer X- and Y- coordinate system. The measured force in X- and Y- direction are translated into tangential (F_t) and radial (F_r) force acting on the tool using Eq. (3).

$$\begin{bmatrix} F_t(t) \\ F_r(t) \end{bmatrix} = \begin{bmatrix} \cos \theta & -\sin \theta \\ \sin \theta & \cos \theta \end{bmatrix} \begin{bmatrix} F_x(t) \\ F_y(t) \end{bmatrix}$$
 (3)

The time instant values of tangential and radial force obtained using Eq. (3) and uncut chip thickness calculated in section 2.1 are fitted in a linear relationships $(F_t(t) = M_t h(t) + C_t, (F_r(t) = M_r h(t) + C_r)$ having slope M_t, M_r and intercept

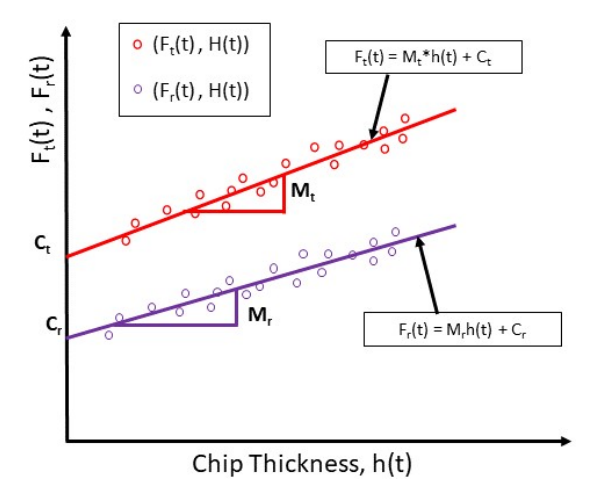


Fig. 1. Linear fitting for determination of cutting and edge force coefficients

 C_t , C_r as depicted in Fig. 1. The linear relationships obtained are compared with Eqs. (1) and (2) and values of cutting and edge coefficients are evaluated using formulation given in Eqs. (4) and (5)

$$K_t = \frac{M_t}{h}, \qquad K_{te} = \frac{C_t}{h} \tag{4}$$

$$K_{t} = \frac{M_{t}}{b}, \qquad K_{te} = \frac{C_{t}}{b}$$

$$K_{r} = \frac{M_{r}}{b}, \qquad K_{re} = \frac{C_{r}}{b}$$
(5)

2.1. Modeling of uncut chip thickness

The basis of developing a mechanistic force model is determining the uncut chip geometry and its thickness. The geometry of the uncut chip varies considerably during slot milling with a trochoidal toolpath due to a combination of circular and linear motion, which is contrary to traditional slot milling having a constant engagement toolpath. Also, the mathematical complexity is higher with trochoidal toolpath and requires a geometrical solution for evaluating chip thickness. The methodology for determining chip thickness has been outlined briefly in this section. However, a detailed explanation can be found in the previous work of authors group [26].

2.1.1. Trochoidal toolpath representation

Trochoidal toolpath is governed by three parameters, firstly, the rotational speed of the tool (θ, RPM) , secondly, revolutionary motion of tool center or nutation rate $(\phi, rad/s)$ and lastly the step over feed rate (v, mm/s). The instantaneous X and Y coordinates traced by the cutting tip of the tool are determined by Eqs. (6) and (7). Fig. 2 depicts the two successive nutations for the 2-fluted trochoidal toolpath. S_w , R_c , t represents slot width, radius of the cutter, and time respectively. In Eqs. (6) and (7), ϕ is a function of feed rate (mm/s) and evaluated using Eq. (8).

$$X_c = (\frac{S_w}{2} - R_c)\cos(\phi t) + R_c\cos(\theta t)$$
 (6)

$$Y_c = (\frac{S_w}{2} - R_c) \sin(\phi t) + R_c \sin(\theta t) + vt$$
 (7)

$$\phi = Feed \ rate \ / \ (\frac{S_w}{2} - R_c) \tag{8}$$

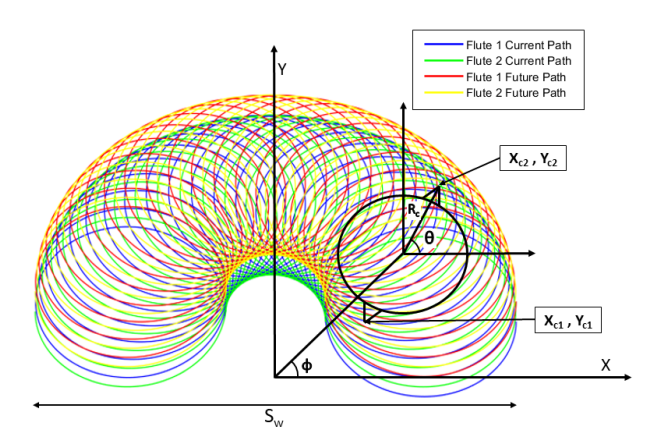


Fig. 2. Trochoidal toolpath for 2-flute cutter (showing 2 successive nutations)

2.1.2. Determination of intersection points

The chip thickness model can be developed by an analytical approach or a numerical approach which relies on developing the chip shape and geometry. The analytical method has some limitations, which have been discussed in the previous work of authors [26], hence, geometrical approach was used. The first step to develop a chip thickness geometry is finding the intersection points between the toolpaths. The chip geometry can be described by a combination of self-intersecting and crossintersecting points in case of a single flute geometry. However, for the 2-fluted toolpath, there will be 4 distinct paths i.e. 2 sets of current and future path, and therefore chip geometry will be described by a combination of cross-intersecting points only.

The circular motion of the tooltip can be discretized into small line segments, and the coordinates of these segments can be determined from the parametric Eqs. (6) and (7). Fig. 3 delineates the basis of the algorithm used to locate the cross-intersection points. A point (X_0, Y_0) on any arbitrary line segment will be considered as a cross-intersection point if the values of ratios L2/L1 and L4/L3 are less than unity. L1 and L3 represents the length of line segments while L2 and L4 represents the distance of (X_0, Y_0) from the farthest point on the line segments. The process is carried out inside a confining rectangle, and the line segments that fall into the bounds are considered at once to achieve a better computational speed. The algorithm locates all the cross-intersection points of the 2-fluted trochoidal toolpath, while the points on the boundary of the current and future path are shown in Fig. 4

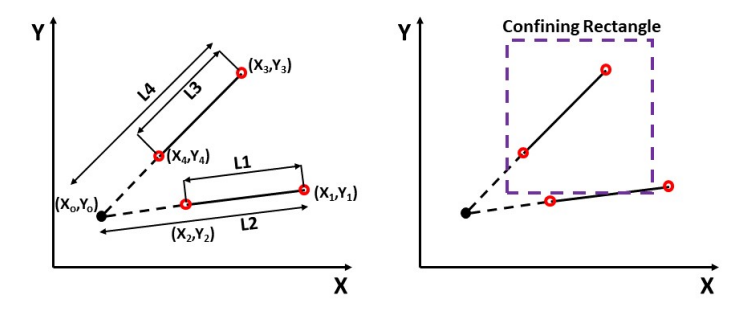


Fig. 3. Geometrical method for extracting cross-intersection points of trochoidal

2.1.3. Evaluation of chip geometry and thickness

The geometry of the chip is defined as an area between the current and future path of the flutes as shown in Fig. 5. For defining chip geometry in the case of a 2-fluted tool, the crossintersection points obtained through the above section are further segregated to construct the outer lobe of the current and future path as shown in Fig. 4. These lobes are constructed by generating a curve encompassing the current and future paths. The points with minimum distance to the encompassing curve were selected (black colored in Fig. 5)and connected to construct the outer lobes. In the further step, the intersection points of the future and current path lying on the outer lobe of the current path were extracted, and only the points lying in the direction of tool motion were selected (magenta colored in Fig. 5) to define

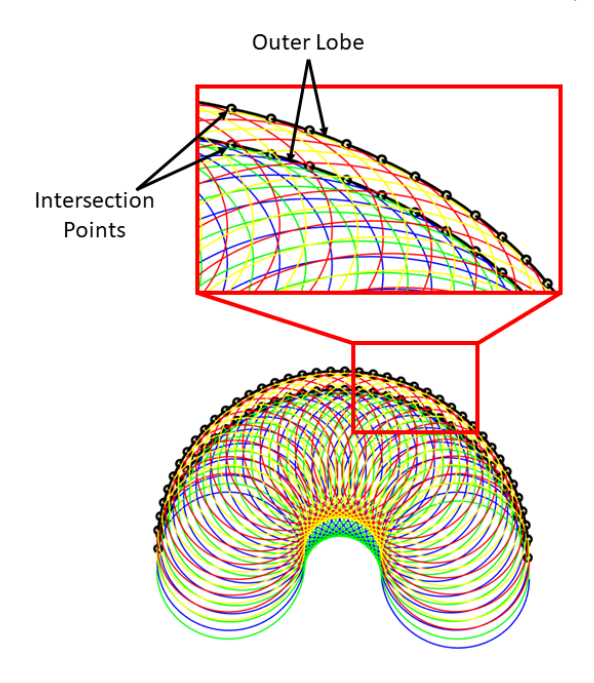


Fig. 4. Intersection points and outer lobe section of trochoidal toolpath

the other bounding points of chip geometry. In the final step, the time indices of intersection points obtained in the above steps are chronologically arranged to trace the boundary of the chips as shown in Fig. 5.

The chip thickness can be defined as the perpendicular distance between the path that the current flute of interest is generating and the exposed work surface that a previously passing

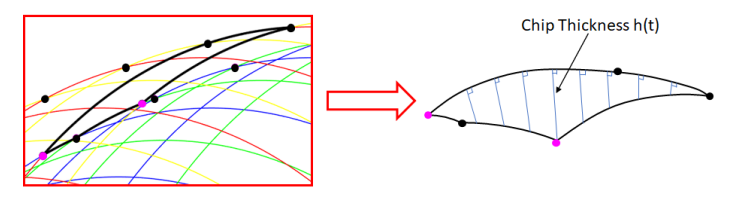


Fig. 5. Geometry and thickness of the chip for trochoidal toolpath

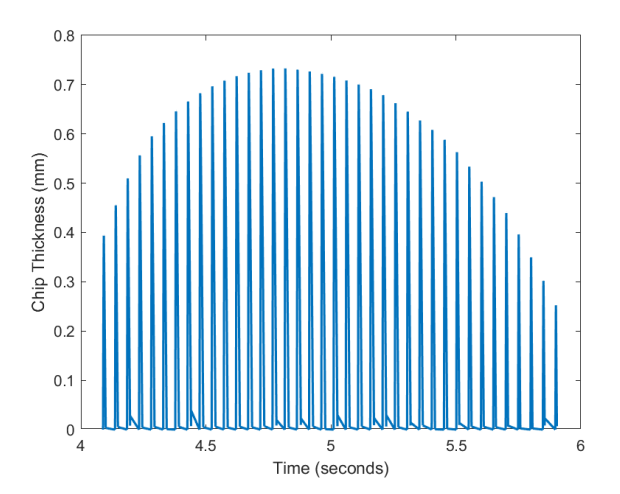


Fig. 6. Chip thickness evolution for one nutation of 2-fluted trochoidal toolpath

flute has generated. Unlike traditional slot milling paths with constant radial engagement, the uncut chip thickness in the trochoidal tool path varies continuously over its nutation because of variable radial engagement. Hence, the chip calculation was accomplished across one complete nutation to capture the entire evolution of chip thickness. The chip thickness for the entire nutation with respect to time was calculated and shown in Fig. 6.

3. Determination of flank wear area

Fig. 7 depicts the overall framework for evaluating the flank wear area. It is an image recognition-based method that processes the microscopic image of tool wear to evaluate the flank wear area of the tool. The detailed methodology has been explained in the previous work of the authors [7] and summarized briefly in this section. At first, the microscopic image of tool wear is processed to eliminate noise, binarized, and extract the boundary of the flank wear area of the tool. In the subsequent step, the cutting edge of the tool is detected to have a reference for the measurement of wear widths. Once the zone of the flank wear area and cutting edge of the tool is identified, the flank wear widths and wear area are measured along the cutting edge. The wear widths were calculated as a length of perpendicular lines overlapping the flank wear area. After that, the trapezoidal integration is applied to evaluate the flank wear area of the tool.

4. Experimental design

The proposed work aims to determine the relationship between edge force coefficients and the flank wear area of the tool. The cutting force measurement is required to determine the edge force coefficient using Eqs. (4) and (5), defined in the above section. Similarly, the tool wear images are needed for the estimation of the flank wear area of the tool. This section outlines the experimental setup for measuring cutting force and capturing wear images of the tool. It also delineates a set of machining experiments conducted at different cutting conditions to establish a relationship between edge force coefficient and flank wear area, and examine its effectiveness.

4.1. Experimental setup for force and wear measurement

A 3-axis CNC vertical milling machine (OKUMA Genos M560-V) and piezo-electric table-mounted dynamometer (Kistler 9257B) were used for conducting machining experiments and recording of cutting force as shown in Fig. 8a). The experiments were performed using a 2-flute indexable end mill and Inconel 718 as workpiece material. The other attributes of the tool and workpiece are summarized in Table 1. The Sandvik carbide inserts (RA390-11 T3 08M-PL S30T) having multilayer coating of TiAlN were inserted into the shoulder mill cutter having a diameter of 15.875 mm. A cylindrical workpiece of 50.8 mm diameter was held in a particular fixture developed as shown in Fig. 8b). The fixture ensures that the workpiece makes contact at four points around the semi-contour of the workpiece. The machinist vise was mounted on the dynamometer to secure

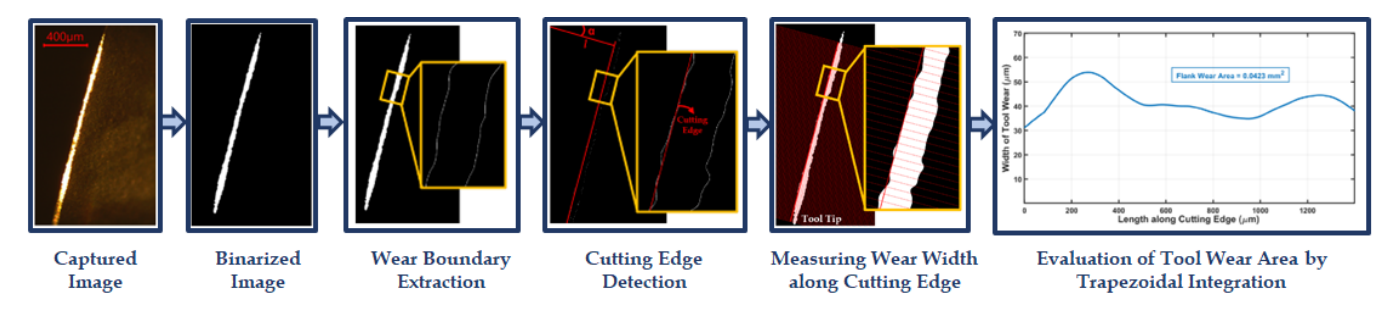


Fig. 7. Overall framework of a image recognition-based evaluation of flank wear area

the workpiece inside the fixture. The machinist vise ensures that pressure is applied downward onto the workpiece, eliminating the chance of the workpiece being pushed upward. A ZEISS Axio Vert.A1 vertical microscope depicted in Fig. 8c) was used to capture microstructural images of the tool for measuring the flank wear area. The tool was mounted on a hollow cylindrical stand and placed over the bed of a vertical microscope to capture the image of inserts.

4.2. Design of experiment

The trochoidal milling experiments were performed at different cutting conditions, summarized in Table 2, to establish a edge force coefficient-based relationship for evaluating the flank wear area of the tool and investigate the efficacy of the developed relationship. The slots having a width of 40 mm were machined using a trochoidal path for every experiment. The machining was performed iteratively with a 1 mm axial depth of cut in each iteration to analyze the effect of tool wear on the values of edge force coefficients. The volume of material removed in each iteration was 842.4 mm³. To study the fully engaged trochoidal milling and isolate the effects of interrupted cuts in the trochoidal path, the initial section of the slot was cleared using another tool, as shown in Fig. 9.

Each experiment was performed using pair of new inserts and continued iteratively till the failure of any of the two inserts was

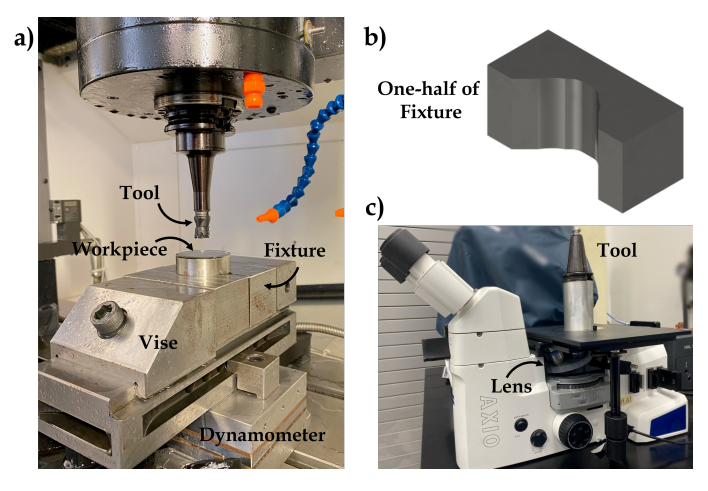


Fig. 8. Experimental setup; (a) Machining setup for trochoidal milling, (b) Onehalf of a fixture, and (c) Vertical microscope to capture tool wear images

Table 1. Tool and Workpiece Attributes						
Tool Attributes (Carbide Indexable End Mill)						
Manufacturer	:	Sandvik				
Catalog Code (Holder)	:	RA390-016EH16-11L				
Catalog Code (Insert)	:	RA390-11 T3 08M-PL S30T				
Cutter Diameter		15.875 mm				
Helix Angle	:	30°				
Lead Angle	:	90°				
No. of Flutes	:	2				
Flute Length	:	10 mm				
Coating	:	TiAlN				
Workpiece Attributes						

Workpiece Attributes					
Material	:	Inconel 718			
Workpiece Shape	:	Round			
Diameter	:	50.8 mm			
Length	:	76.2 mm			

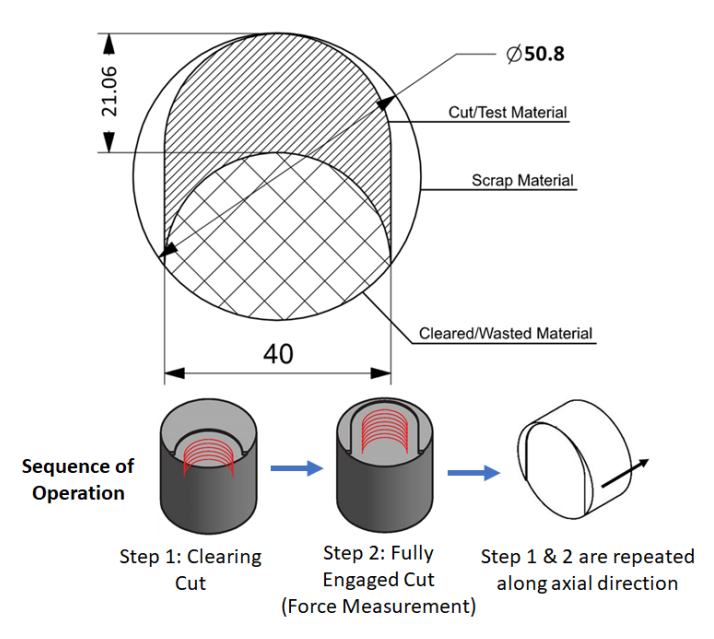


Fig. 9. Workpiece attributes and Sequence of operation

observed. For each iteration, the in-process cutting forces were recorded as shown in Fig. 11, and the tool wear images were captured (after completion of iteration). The workpiece was slightly raised after each iteration, and height was measured using an

On-Machine Measuring (OMM) probe. A facing operation was performed between the two iterations to remove the unmachined material of the previous iteration. The process can be assumed repeatable owing to the application of the OMM probe. A synthetic coolant with flood flow and 8.5% concentration was used during the machining experiments.

Table 2. Design of Experiments

Test No.	Surface Speed	S_1	pindle Speed	Iteration	
	(m/min)		(RPM)	Completed	
1	60		1203	11	
2	45		902	14	
3	25		501	25	
Step over fe	eed rate (v)	:	0.25 mm/s		
Axial Deptl	h of Cut	:	1 mm		
Feed per To	ooth	:	0.25 mm/too	oth	
Slot Width		:	40 mm		
Volume Removed per Iteration		:	$842.4 \ mm^3$		
Coolant Flo)W	:	Flood		
Coolant Co	ncentration	:	8.5 %		

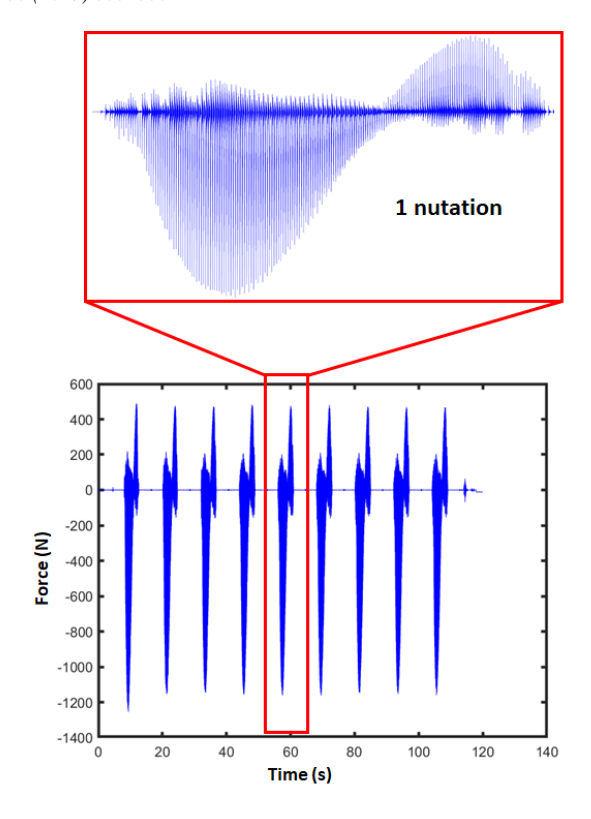


Fig. 11. Experimental force measured for one iteration

5. Relation of edge force coefficients and flank wear area

This section uses the cutting condition corresponding to test 1 of Table 2 to calibrate the relationship between edge force coefficients and flank wear area. As discussed in section 4.2, multiple iterations of machining were carried out until chipping occurred at any of the two inserts, and the tool became nonfunctional. Each iteration of an experiment consists of nine trochoidal nutations as represented in Fig. 11 by nine sets of force. However, the calculation for edge force coefficients and flank wear area of the tool was done for a 5th nutation only. The reason for selecting 5th nutation is that it represents the cutting force at the middle of the cut. Thereafter, the edge force coefficients and flank wear area were evaluated for other iteration and plotted against the volume of material removed, discussed in the section 5.1. Eventually, the relationship between edge force coefficients and tool wear area is developed in section 5.2.

5.1. Evolution of edge force coefficient and tool wear area

The values of in-process edge force coefficients (k_{te} , k_{re}) were calculated using Eqs. (4) and (5) as explained in Section 2. Similarly, the values of the flank wear area of the tool were evaluated using image recognition-based methodology explained in Section 3. These values were continuously tracked for the entire duration of the span life of the tool. The failure of the tool was observed during 12^{th} iteration in the case of test 1. Fig. 10 depict the evolution of k_{te} , k_{re} and flank wear area (W_{flank}) plotted over the volume of material removed before tool failure (11 iterations). It is observed that the evolution of edge force coefficients mimics the three wear stages of the tool, namely (a) initial region, (b) steady-state region, and (c) failure region. Therefore, it can be concluded that k_{te} , k_{re} are sensitive to the tool health parameters and can be used to estimate the flank wear area of the tool.

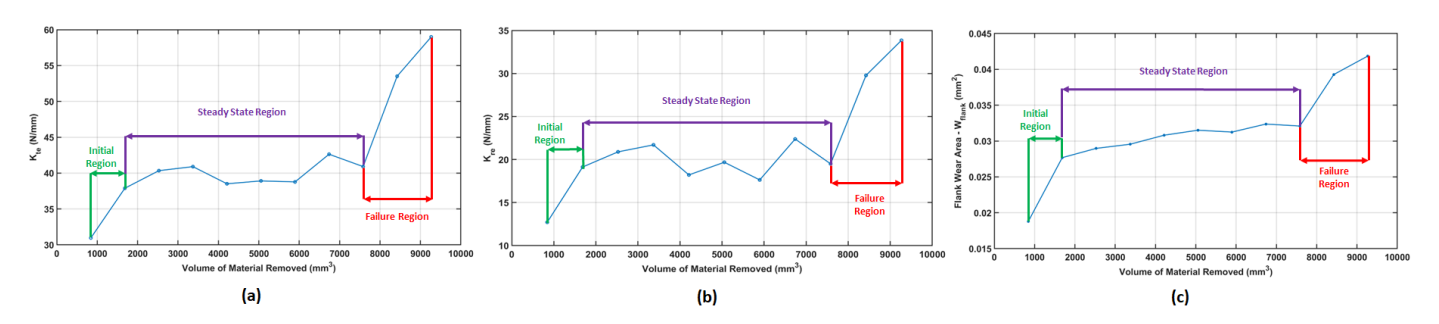


Fig. 10. Evolution of (a) k_{te} and (b) K_{re} and (c) W_{flank} with volume of material removed

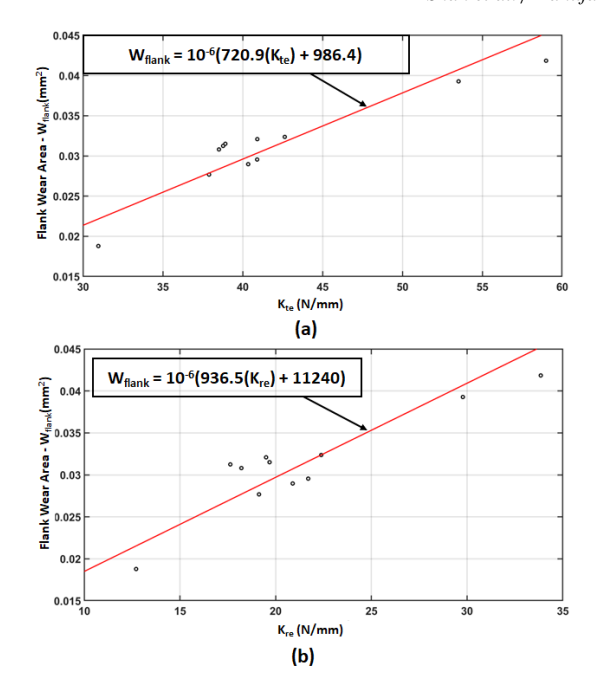


Fig. 12. (a) Linear Fit between K_{te} and W_{flank} (b) Linear Fit between K_{re} and W_{flank}

5.2. Calibration of relationship

The values of edge coefficients (K_{te} , K_{re}) and flank wear area (W_{flank}) evaluated as a function of volume of material removed are further used to calibrate the required relationship. The curve fitting technique was applied to derive the formulation for flank wear estimator, as expressed in Eqs. (9) and (10). Fig. 12a and b show the linear relationship obtained along with the values of slope and intercept. The R-square value for K_{te} Vs W_{flank} was 0.8749 and that for K_{re} vs W_{flank} was 0.8355, indicating that a linear fit is good and accurate enough to predict flank wear area.

$$W_{flank} = 10^{-6} (720.9 K_{te} + 986.4) \tag{9}$$

$$W_{flank} = 10^{-6} (936.5 K_{re} + 11240) \tag{10}$$

6. Experimental validation

The effectiveness of the relationship formulated for evaluating the flank wear area of the tool is examined by conducting a slot milling experiment with a trochoidal toolpath for the cutting condition summarized in Table 2 (Test 2 and 3). These tests aim to assess the prediction accuracy of the proposed indirect approach for measuring flank wear area over the range of surface speeds. The flank wear area is estimated using relationships expressed in Eqs. (9) and (10) and compared subsequently with experimentally measured values using an image recognition-based methodology outlined in section 3.

Fig. 13 shows the comparative assessment of flank wear area predicted indirectly using developed k_{te} and K_{re} based relationship and experimentally corresponding to the cutting condition presented in test 2 (Table 2). It can be observed that K_{te} based

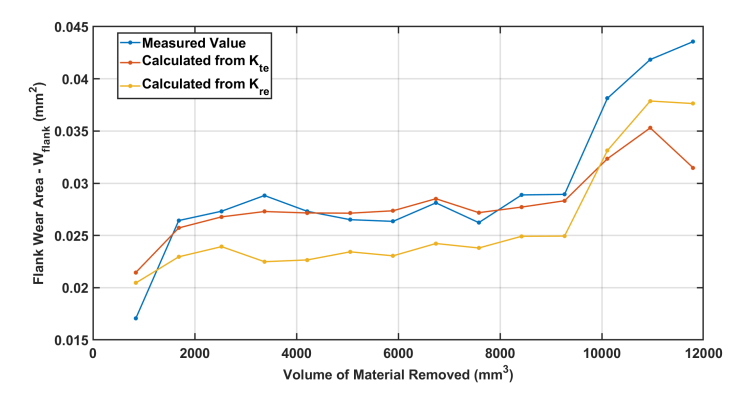


Fig. 13. Comparison of measured and calculated flank wear area (Test 2)

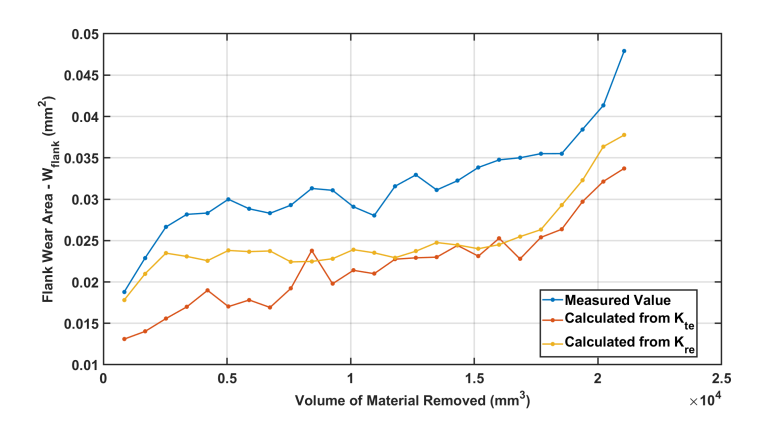


Fig. 14. Comparison of measured and calculated flank wear area (Test 3)

relationship evaluates the profile and magnitude of flank wear values very close to experimental values for test 2 in the initial and steady region. However, in the failure region, the flank wear area values are predicted lesser than the experimental values. The lower prediction accuracy in the failure region can be attributed to the highly stochastic nature of the wear phenomenon in this region, which leads to a poor approximation of the relationship. Further, the K_{re} based relationship accurately follows the three-region profile of flank wear area, but the magnitude is predicted consistently lower, which needs further investigation. Similarly, Fig. 14 shows the comparative assessment of flank wear area for the cutting conditions presented in test 3. Here, it is observed that both K_{te} and K_{re} based relationship follows the three-region profile of wear but lacks accuracy while predicting the magnitude of flank wear area. This can be attributed to the significant difference in surface speed value used for formulating and validating the relationship. The accuracy can be improved by conducting more experiments to develop the relationships. Based on the outcome, it can be presumed that the proposed approach can effectively measure the tool's in-process flank wear area, thereby eliminating the need to interrupt the cutting operation to monitor the tool condition. However, further validation can be performed over range of cutting parameters to confirm the applicability of this approach.

7. Conclusion and future work

This paper formulates edge force coefficient-based linear relationships to estimate the flank wear area of the tool during trochoidal milling of Inconel 718. The relationships developed are substantiated by conducting slot milling experiments using trochoidal toolpath over a range of surface speeds. It can be concluded that an effective linear relationship can be formed between edge coefficients and the flank wear area of the tool. The experimental validation of the developed relationship indicates that the edge force coefficients can effectively indicate tool condition and reasonably measure the value of the flank wear area. However, the relationships developed in the present study can be improved further by increasing the number of experiments used for formulating relationships and captures the effect of other parameters. In future work, the proposed relationships can be incorporated into the controller of the machine setup to predict the flank tool wear area with cutting force as an input. Incorporating an in-process flank tool wear area can assist manufacturers or operators in estimating tool conditions without interrupting the machining process and removing the tool.

Acknowledgements

The investigations are based on the research project "Stochastic Modeling of the Interaction of Tool Wear and the Machining Affected Zone in Nickel-Based Superalloys", which is kindly funded by the National Science Foundation under Grant No. 1760809.

References

- [1] Potthoff, N., Agarwal, A., Wöste, F., Liß, J., Mears, L., Wiederkehr, P., 2022. Experimental and simulative analysis of an adapted methodology for decoupling tool wear in end milling. Manufacturing Letters 33, 380–387.
- [2] Pleta, A., Ulutan, D., Mears, L., 2014. Investigation of trochoidal milling in nickel-based superalloy inconel 738 and comparison with end milling, in: International manufacturing science and engineering conference, American Society of Mechanical Engineers. p. V002T02A058.
- [3] Altin, A., Nalbant, M., Taskesen, A., 2007. The effects of cutting speed on tool wear and tool life when machining inconel 718 with ceramic tools. Materials & design 28, 2518–2522.
- [4] Hadi, M., Ghani, J., Haron, C.C., Kasim, M., 2013. Comparison between up-milling and down-milling operations on tool wear in milling inconel 718. Procedia Engineering 68, 647–653.
- [5] Zhaoyu, L., Pengcheng, H., Fubao, X., Kai, T., 2021. A variable-depth multilayer five-axis trochoidal milling method for machining deep freeform 3d slots. Robotics and Computer-Integrated Manufacturing 68, 102093.
- [6] Hou, Q., Sun, J., Huang, P., 2019. A novel algorithm for tool wear online inspection based on machine vision. The International Journal of Advanced Manufacturing Technology 101, 2415–2423.
- [7] Agarwal, A., Potthoff, N., Shah, A.M., Mears, L., Wiederkehr, P., 2022. Analyzing the evolution of tool wear area in trochoidal milling of inconel 718 using image processing methodology. Manufacturing Letters 33, 373– 379.
- [8] Kurada, S., Bradley, C., 1997. A machine vision system for tool wear assessment. Tribology International 30, 295–304.
- [9] Yu, J., Cheng, X., Lu, L., Wu, B., 2021. A machine vision method for measurement of machining tool wear. Measurement 182, 109683.

- [10] Kaya, B., Oysu, C., Ertunc, H.M., 2011. Force-torque based on-line tool wear estimation system for cnc milling of inconel 718 using neural networks. Advances in Engineering Software 42, 76–84.
- [11] Stavropoulos, P., Papacharalampopoulos, A., Souflas, T., 2020. Indirect online tool wear monitoring and model-based identification of process-related signal. Advances in Mechanical Engineering 12, 1687814020919209.
- [12] Li, T., Shi, T., Tang, Z., Liao, G., Duan, J., Han, J., He, Z., 2021. Real-time tool wear monitoring using thin-film thermocouple. Journal of Materials Processing Technology 288, 116901.
- [13] Shao, H., Wang, H., Zhao, X., 2004. A cutting power model for tool wear monitoring in milling. International Journal of Machine Tools and Manufacture 44, 1503–1509.
- [14] Zhang, X., Wang, S., Li, W., Lu, X., 2021. Heterogeneous sensors-based feature optimisation and deep learning for tool wear prediction. The International Journal of Advanced Manufacturing Technology 114, 2651–2675.
- [15] Binsaeid, S., Asfour, S., Cho, S., Onar, A., 2009. Machine ensemble approach for simultaneous detection of transient and gradual abnormalities in end milling using multisensor fusion. Journal of Materials Processing Technology 209, 4728–4738.
- [16] Liao, Z., Gao, D., Lu, Y., Lv, Z., 2016. Multi-scale hybrid hmm for tool wear condition monitoring. The International Journal of Advanced Manufacturing Technology 84, 2437–2448.
- [17] Pleta, A., Niaki, F.A., Mears, L., 2017. Investigation of chip thickness and force modelling of trochoidal milling. Procedia Manufacturing 10, 612–621.
- [18] Agarwal, A., Desai, K., 2020. Importance of bottom and flank edges in force models for flat-end milling operation. The International Journal of Advanced Manufacturing Technology 107, 1437–1449.
- [19] Choudhury, S., Rath, S., 2000. In-process tool wear estimation in milling using cutting force model. Journal of Materials Processing Technology 99, 113–119.
- [20] Cui, Y., 2008. Tool wear monitoring for milling by tracking cutting force model coefficients. University of New Hampshire.
- [21] Nouri, M., Fussell, B.K., Ziniti, B.L., Linder, E., 2015. Real-time tool wear monitoring in milling using a cutting condition independent method. International Journal of Machine Tools and Manufacture 89, 1–13.
- [22] Zhou, Y., Sun, W., 2020. Tool wear condition monitoring in milling process based on current sensors. IEEE Access 8, 95491–95502.
- [23] Liu, Y.P., Kilic, Z.M., Altintas, Y., 2022. Monitoring of in-process force coefficients and tool wear. CIRP Journal of Manufacturing Science and Technology 38, 105–119.
- [24] Luo, H., Zhang, Z., Luo, M., Zhang, D., 2022. A comparative study of force models in monitoring the flank wear using the cutting force coefficients. Proceedings of the Institution of Mechanical Engineers, Part C: Journal of Mechanical Engineering Science, 09544062221111706.
- [25] Pleta, A., Niaki, F.A., Mears, L., 2018. A comparative study on the cutting force coefficient identification between trochoidal and slot milling. Procedia Manufacturing 26, 570–579.
- [26] Akhavan Niaki, F., Pleta, A., Mears, L., 2018. Trochoidal milling: investigation of a new approach on uncut chip thickness modeling and cutting force simulation in an alternative path planning strategy. The International Journal of Advanced Manufacturing Technology 97, 641–656.